technologies

MDPI

Article

Additive Manufacturing: Reproducibility of Metallic Parts

Konda Gokuldoss Prashanth [1,*], Sergio Scudino [2], Riddhi P. Chatterjee [2], Omar O. Salman [2] and Jürgen Eckert [1,3]

[1] Erich Schmid Institute of Materials Science, Austrian Academy of Sciences, Jahnstraße 12, A-8700 Leoben, Austria; juergen.eckert@unileoben.ac.at
[2] IFW Dresden, Institute for Complex Materials, Postfach 270116, D-01171 Dresden, Germany; s.scudino@ifw-dresden.de (S.S.); riddhipratim.chatterjee@gmail.com (R.P.C.); o.o.salman@ifw-dresden.de (O.O.S)
[3] Department Materials Physics, Montanuniversität Leoben, Jahnstraße 12, A-8700 Leoben, Austria
* Correspondence: kgprashanth@gmail.com or Prashanth.kondagokuldoss@oeaw.ac.at; Tel.: +43-3842-804-206; Fax: +43-3482-804-116

Academic Editors: Salvatore Brischetto, Paolo Maggiore, Carlo Giovanni Ferro and Manoj Gupta
Received: 20 December 2016; Accepted: 18 February 2017; Published: 22 February 2017

Abstract: The present study deals with the properties of five different metals/alloys (Al-12Si, Cu-10Sn and 316L—face centered cubic structure, CoCrMo and commercially pure Ti (CP-Ti)—hexagonal closed packed structure) fabricated by selective laser melting. The room temperature tensile properties of Al-12Si samples show good consistency in results within the experimental errors. Similar reproducible results were observed for sliding wear and corrosion experiments. The other metal/alloy systems also show repeatable tensile properties, with the tensile curves overlapping until the yield point. The curves may then follow the same path or show a marginal deviation (~10 MPa) until they reach the ultimate tensile strength and a negligible difference in ductility levels (of ~0.3%) is observed between the samples. The results show that selective laser melting is a reliable fabrication method to produce metallic materials with consistent and reproducible properties.

Keywords: selective laser melting; laser processing; metals and alloys; mechanical properties; tensile properties

1. Introduction

Ever since the manufacturing of materials took place in the Bronze Age, the existing techniques have been constantly developed and new manufacturing processes have been invented [1]. Conventional casting and powder metallurgy (powder production followed by consolidation) are two widely used manufacturing processes to produce parts for different applications [2–5]. Even though these processes are widely used, there are several problems associated with them. For example, the parts fabricated by conventional casting processes may tend to have one of the following processing defects: surface defects, internal defects, inconsistency in chemical composition (segregation) and/or unsatisfactory mechanical properties (inconsistencies in the grain structure) [6]. Similarly, the parts manufactured by powder metallurgy may have defects introduced at various stages during the fabrication chain, such as powder production (non-uniform chemical composition), powder compaction (porosity) and sintering (porosity and oxidation of surface) [7,8]. Defects can also originate during post-processing of the parts after fabrication [7]. All these defects, which are introduced at different stages of manufacturing or post-processing may lead to inferior/inconsistency in properties [9,10]. However, the stringent industrial regulations (automobile, aeronautical, power plants and nuclear industry) nowadays require parts to have highly reproducible mechanical properties [11].

To conform to the stringent regulations, efforts have been made to find alternative processing routes or to reduce the unreliability factor in the existing processing capabilities. Additive manufacturing is seen as one of the viable alternative processing routes which may lead to consistent properties in materials. The laser-based powder bed fusion process (ISO/ASTM52900:2015 Standard Terminology for Additive Manufacturing–General Principles–Terminology), which is commonly known as Selective Laser Melting (SLM) is one of the additive manufacturing processes, which produces three-dimensional metal parts layer by layer with superior properties compared to conventional manufacturing processes such as casting and powder metallurgy [12–15]. A suitable combination of the processing parameters such as the laser power, laser scan speed, hatch distance, hatch style, layer thickness and laser spot size leads to the fabrication of a defect-free component by SLM [12]. The above-mentioned parameters, with the exception of hatch style, determine the heat/energy supplied to the powder bed (heat/energy input). The amount of powder surface exposed to the laser during the SLM process is rather small and hence a very high energy density is involved during the SLM process. This intense energy input leads to very high cooling rates observed in the rate of ~10^5–10^6 K/s [16,17]. Such high cooling rates will result in substantially refined microstructures compared to the conventional manufacturing processes, and hence improved properties [16,17].

The majority of the research on the SLM process is focused on parameter optimization, alloy development, topology optimization/structure optimization and microstructure-property correlation. The intent of the present manuscript is to highlight the repeatability/reproducibility aspects of the samples produced by SLM in terms of the material properties. Five different materials—Al-12Si, Cu-10Sn, and 316L, belonging to the face-centered cubic structure, CoCrMo and CP-Ti with hexagonal closed packed structure—were evaluated and their properties are reported to show consistency in the properties of the samples produced by SLM.

2. Experimental Section

Cylindrical tensile samples (total length 52 mm, length and diameter of the gauge length 17.5 and 3.5 mm) were fabricated from spherical gas-atomized powders at room temperature using an SLM 250 HL device (from SLM Solutions and formerly Machine Tool Technologies Solutions). The device is equipped with a Yb-YAG laser. All the samples were built over a base plate made of the same material as the building material under an Ar environment (in order to avoid oxygen contamination during the building process) with a hatch style rotation of 73°. Hatch style is defined as the design/pattern in which the hatches (melting sequences or melt lines or melt tracks) are oriented within and between the layers [18]. Detailed information about the hatch style can be found in [19]. All the samples were built perpendicular to the base plate (i.e., *XY* direction). An allowance of 1–2 mm was given for these samples, so that they can be machined with the abrasive papers to smoothen their surface before the tensile test. The tensile test samples used in the present study were selected randomly from different batches at randomly built positions in the substrate plate, in order to ascertain the reproducibility criteria and were used in the as-built condition. The Al-12Si samples (from gas atomized powder with a nominal composition of Al-12Si (wt.%)) were fabricated with a laser power of 320 W for both the bulk of the sample and the contour and the laser scan speed of 1455 mm/s for the bulk and 1939 mm/s for the contour. A layer thickness of 50 μm is used with a laser spot size of ~80 μm and a hatch distance of ~110 μm. Detailed information about the fabrication of the Al-12Si samples can be found elsewhere [20]. The following parameters were used for the fabrication of CoCrMo parts (from CoCrMo gas atomized powder from SLM solutions): laser power—100 W; laser scan speed—140 mm/sec; layer thickness—30 μm; and hatch distance—100 μm, with 90° hatch rotation between the layers [21]. For further processing details about CoCrMo, see [21]. Commercially pure Ti (CP-Ti) samples were built from CP-Ti grade 2 powder supplied by TLS Technik GmbH, Germany with the following parameters: laser power—165 W; laser scan speed—138 mm/s; layer thickness—100 μm; and hatch distance—100 μm, with 90° hatch rotation between the layers. Detailed information about the fabrication of the CP-Ti can be found at [22]. Gas atomized 316L powders were used to fabricate

SLM parts with the following parameters: laser power—100 W; laser scan speed—800 mm/s; layer thickness—30 μm; and hatch distance—120 μm, with 90° hatch rotation between the layers [23,24]. Similar gas atomized bronze powders (with the following parameters: laser power—271 W; laser scan speed—210 mm/s; laser thickness—90 μm; and hatch distance—90 μm) were used for producing the bulk SLM bronze parts [25]. Cylindrical bulk samples were also prepared by graphite mold casting in order to compare the properties of the conventionally fabricated cast samples with the SLM samples. Room temperature tensile tests were carried out using an Instron 8562 testing facility (strain rate $1 \times 10^{-4}\ s^{-1}$) and the strain during the tensile test was measured directly on the specimen using a Fiedler laser-extensometer. At least three specimens were tested under each condition to ascertain the reproducibility/repeatability of the properties. The wear and corrosion test conditions have been reported elsewhere [26]. For the corrosion experiments, the samples were mounted in polymer resin and are polished metallographically to mirror finish. A Solarton SI Electrochemical Interface connected to a tempered three-electrode-cell with a Pt net as the counter electrode was used, with a saturated calomel reference electrode (SCE with Standard Hydrogen Electrode potential E_{SHE} = 0.241 V at room temperature) and the embedded alloy sample as the working electrode. Before the actual polarization measurements, the samples were kept at open circuit potential (OCP) conditions for 1 h; meanwhile, the potential was monitored. The linear dynamic polarization was started at −0.2 V vs. OCP, and the potential was increased at a constant rate of 0.5 mV/s up to a value of 1.5 V vs. SCE.

3. Results and Discussion

Figure 1 shows the room temperature tensile curves of the Al-12Si samples manufactured by SLM and the corresponding mechanical data are summarized in Table 1. The tensile curves (in color) in Figure 1a show the consolidated data of six tensile tests that are shown individually in Figure 1b. It is observed from Figure 1a that all the six tensile curves almost overlap one another and only negligible differences are observed after yielding and at the time of fracture. The yield strength (YS) of these six samples varies between 239 and 242 MPa and the ultimate tensile strength (UTS) varies between 375 and 384 MPa. The ductility of the sample varies between 2.65% and 2.85%, showing consistency in the tensile properties. Zhang et al. and Li et al. have also shown that tensile properties of Al-12Si samples prepared by SLM under Ar atmosphere lie in the range: YS—235 and 250 MPa; UTS—370 and 390 MPa; and ductility 2.75% and 3% [27,28]. Interestingly, both Zhang et al. and Li et al. fabricated the Al-12Si samples with the SLM device from ReaLizer and not from SLM solutions. Siddique et al. has also produced Al-12Si samples by SLM using the SLM solutions device and the tensile properties lie within the above said range [29]. This suggests that with the optimized parameters for full density, the Al-12Si SLM samples will show repeatable/reproducible tensile properties within the experimental errors. However, there are reports of anisotropy in the SLM produced samples and the mechanical properties vary depending on the building direction [30–33]. Alsalla et al. have shown that the tensile strength and the fracture toughness of the 316L cellular lattice manufactured by the SLM technique, depends greatly on the building direction. This is essentially due to the anisotropic behavior of the SLM-prepared samples [30]. Similar anisotropy has been reported by Suryawanshi et al., where the fracture toughness of the Al-12Si samples depends strongly on the building direction [17]. On the other hand, some results also suggest that the sample building direction does not have a significant effect on the tensile properties [20]. Hence, there exists a contradiction between the consistencies in the tensile properties of samples prepared with different build orientation. However, it may be safe to say that even if there is a difference in properties between the samples prepared with different build directions, the differences are consistent and reproducible within the experimental limits. This suggests that the samples built in each orientation (*XY*/*YZ*/*XZ*) should give repeatable and reproducible mechanical properties, when tested in similar conditions.

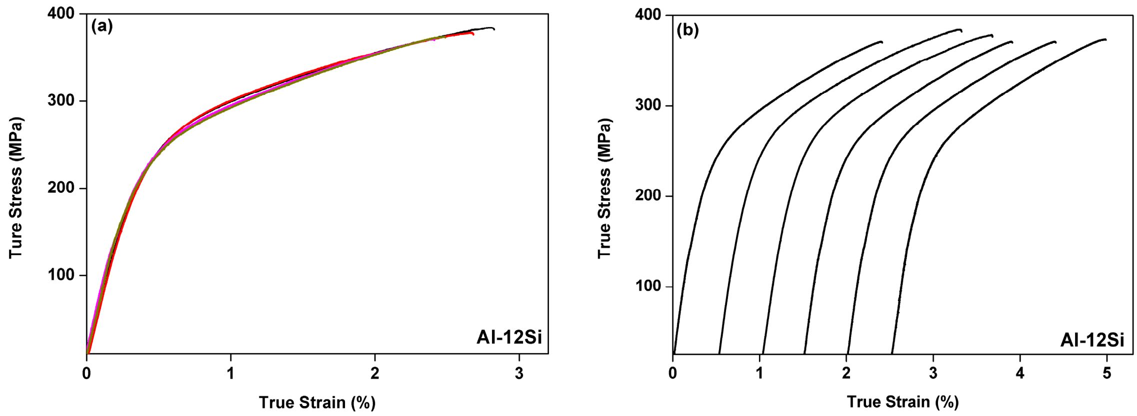

Figure 1. Room temperature tensile test curves for the Al-12Si SLM samples (**a**) consolidated data; (**b**) individual tensile curves.

Table 1. Tensile properties of samples produced by selective laser melting (SLM) and casting (cast).

Properties \ Samples Designation	Al-12Si—SLM	Al-12Si—Cast	316L—SLM	316L—Cast	CoCrMo—SLM	CoCrMo—Cast
Yield Strength (MPa)	240 ± 1	62 ± 9	495 ± 3	254 ± 45	764 ± 2	621 ± 22
Ultimate Tensile Strength (MPa)	380 ± 4	166 ± 48	836 ± 7	573 ± 56	1201 ± 10	908 ± 55
Fracture strain (%)	2.8 ± 0.1	10 ± 4	35.0 ± 0.5	18 ± 6	12.7 ± 0.5	5.8 ± 2

The sliding wear test data of Al-12Si SLM samples are shown in Figure 2a. The data points (corresponding to sample number 1) are the consolidated data points of six sliding wear test experiments that are shown as samples 2–7 (Figure 2a). The wear test results are quite repeatable with the wear rate varying between 9.23 and 9.24 × 10^{-13} m^3/m, showing consistency within the experimental errors. Similar results have been observed for the corrosion studies (conducted in an acidic HNO_3 medium), where the potentiodynamic polarization curves between two test samples almost overlap each other except for small but negligible differences within the experimental limits (Figure 2b). The above results indicate that the tensile properties, wear rate and potentiodynamic corrosion results obtained for the Al-12Si samples produced by SLM are very consistent and reproducible in nature. It might be thought that the Al-12Si samples show consistent and reproducible properties because both Al and Si phases constituting the structure have a face centered cubic (fcc) crystal structure. Hence, to further check the reproducibility of the mechanical properties of SLM parts, other fcc systems such as Cu-10Sn bronze and 316L (predominantly austenite phase) and hexagonally closed packed (hcp) systems, CoCrMo and commercially pure Ti (CP-Ti), were evaluated.

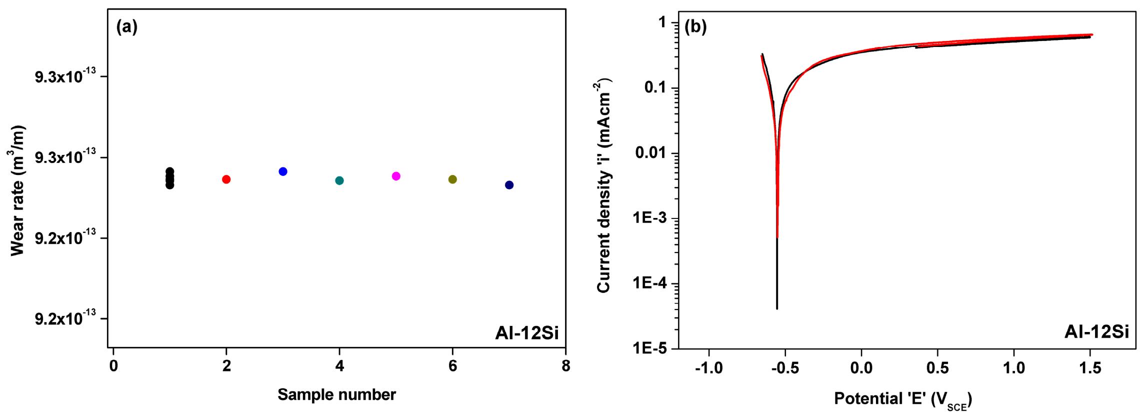

Figure 2. (**a**) Wear rate data for Al-12Si samples carried out at 10 N load; (**b**) Potentiodynamic polarization curves of Al-12Si SLM samples measured in acidic 1 M HNO_3 (pH = 0).

Figure 3 shows the room temperature tensile tests for CoCrMo, 316L, commercially pure Ti (CP-Ti) and Cu-10Sn bronze alloys. Two tensile curves for each alloy are shown in a consolidated fashion (in color) followed by their individual tensile curves (in black). The consolidated curves for Cu-10Sn overlap and no significant differences are found from the tensile test results. A similar trend is observed for the 316L samples, where a marginal difference of ~8 MPa in YS is realized between two tensile tests along with a difference in UTS of ~15 MPa and ductility of ~0.3%. The tensile test curves for CP-Ti do not show any difference in YS between two tensile test results and a marginal difference in UTS and ductility of ~5 MPa and ~0.3%, respectively, is observed. Similar results were found in the case of the SLM-processed CoCrMo alloy. The alloy shows a difference of ~1 MPa in YS between two tensile test results and the difference between the UTS and ductility is ~9 MPa and ~0.45%, respectively. The tensile properties of the Al-12Si, 316L and CoCrMo samples fabricated by casting are shown in Table 1. It can be observed that the samples fabricated by casting have inferior strengths. Moreover, the cast samples show a larger standard deviation compared to the samples fabricated by SLM. The above results from different alloy systems reveal that the SLM-processed materials show very good consistency in their properties (mechanical, tribological and corrosion properties) within the experimental errors, even though the samples were picked randomly from several batches (8–10 batches over 1 year in the case of Al-12Si). The placement of the sample during the building process was also selected randomly. The results were conclusive that the sample batches, irrespective of the sample position, will yield similar, consistent and reproducible properties, if the hardware remains the same along with the quality of the laser. This is because the same hardware with the same quality of laser source will yield a similar amount of defects (porosity level) and hence similar or reproducible properties. This suggests that the SLM process can lead to the production of metals and alloys with superior as well as more reproducible properties compared to their counterparts produced by conventional casting.

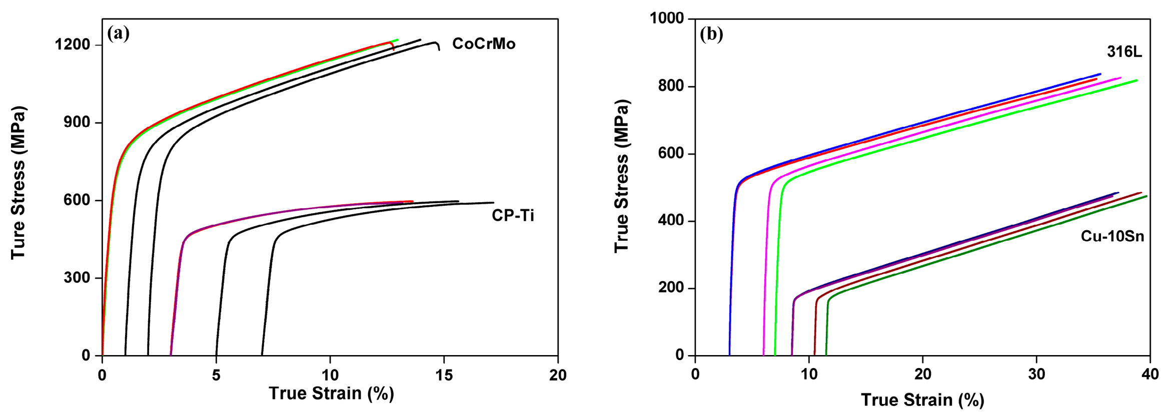

Figure 3. Room temperature tensile curves for (**a**) CoCrMo and commercially pure Ti (CP-Ti) and (**b**) 316L and Cu-10Sn bronze materials.

4. Conclusions

Five different metal/alloy systems (Al-12Si, Cu-10Sn and 316L—face centered cubic phase and CoCrMo and CP-Ti—hexagonal closed packed phase) were fabricated by SLM using commercially available parameters. The Al-12Si fcc samples show uniform and consistent mechanical, tribological and corrosion properties within the experimental errors. It is noteworthy that the room temperature tensile curves overlap one another up to the yield point and show similar behavior, beyond yielding or marginal differences in the ultimate tensile strength (difference ~10 MPa) and/or ductility (~0.2%), thus demonstrating the reliability of the samples fabricated by SLM. Similar tensile results were observed in the case of the other four metal/alloy systems (Cu-10Sn, 316L, CoCrMo and CP-Ti), where the room temperature curves show consistency in their mechanical properties. These results suggest that the selective laser melting process can be used to produce parts with consistent and reproducible properties, provided the powder quality and the parameters for fabrication remain the same.

Acknowledgments: The authors would like to thank A. Gebert for providing the facilities to carry out the corrosion experiments and for stimulating technical discussions. Financial support through the German Science Foundation (DFG) under the Leibniz Program (grant EC 111/26-1) and the European Research Council under the ERC Advanced Grant INTELHYB (grant ERC-2013-ADG-340025) is gratefully acknowledged.

Author Contributions: Konda Gokuldoss Prashanth, Sergio Scudino, and Jürgen Eckert conceived and designed the experiments; Konda Gokuldoss Prashanth performed the experiments on Al-12Si, Ti and Cu-10Sn alloys; Omar O. Salman performed the experiments on 316L and Riddhi P. Chatterjee on CoCrMo alloys. Konda Gokuldoss Prashanth and Sergio Scudino analyzed the data; all the authors have contributed to the discussion of the results and the writing of the paper.

Conflicts of Interest: The authors declare no conflict of interest.

References

1. Historical Development of Materials and Manufacturing Process. 2016. Available online: http://me-mechanicalengineering.com/historical-development-of-materials-and-manufacturing-process/ (accessed on 15 June 2016).
2. Groover, M.P. *Introduction to Manufacturing Processes*; John Wiley & Sons: New York, NY, USA, 2012.
3. Shercliff, H.R.; Lovatt, A.M. Selection of manufacturing processes in design and the role of process modelling. *Prog. Mater. Sci.* **2001**, *46*, 429–459. [CrossRef]
4. Wang, Z.; Prashanth, K.G.; Chaubey, A.K.; Löber, L.; Schimansky, F.P.; Pyczak, F.; Zhang, W.W.; Scudino, S.; Eckert, J. Tensile properties of Al-12Si matrix composites reinforced with Ti-Al based particles. *J. Alloys Compd.* **2015**, *630*, 256–259. [CrossRef]
5. Wang, Z.; Prashanth, K.G.; Scudino, S.; Chaubey, A.K.; Sordelet, D.J.; Zhang, W.W.; Li, Y.Y.; Ecker, J. Tensile properties of Al matrix composites reinforced with in situ devitrified $Al_{84}Gd_6Ni_7Co_3$ glassy particles. *J. Alloys Compd.* **2014**, *586*, S419–S422. [CrossRef]
6. Rajkolhe, R.; Khan, J.G. Defects, causes and their remedies in casting process: A review. *Int. J. Res. Advent Technol.* **2014**, *2*, 375–383.
7. Gutmanas, E.Y. Materials with fine microstructures by advanced powder metallurgy. *Prog. Mater. Sci.* **1990**, *34*, 261–366. [CrossRef]
8. Khan, M.I.; Haque, S. *Manufacturing Science*; PHI Learning Private Limited: New Delhi, India, 2011.
9. Wang, H.T.; Fang, Z.G.Z.; Sun, P. A critical review of mechanical properties of powder metallurgy titanium. *Int. J. Powder Metall.* **2010**, *46*, 45–57.
10. Klar, E.; Samal, P. *Powder Metallurgy Stainless Steels: Processing, Microstructures and Properties*; ASM International: Materials Park, Ohio, USA, 2007.
11. Pandiripalli, B. *Repeatability and Reproducibility Studies: A Comparison of Techniques*; Wichita State University: Wichita, KS, USA, 2010.
12. Olakanmi, E.O.; Cochrane, R.F.; Dalgarno, K.W. A review on selective laser sintering/melting (SLS/SLM) of aluminium alloy powders: Processing, microstructure and mechanical properties. *Prog. Mater. Sci.* **2015**, *74*, 401–477. [CrossRef]
13. Prashanth, K.G.; Shahabi, H.S.; Attar, H.; Srivastava, V.C.; Ellendt, N.; Uhlenwinkel, V.; Eckert, J.; Scudino, S. Production of high strength $Al_{85}Nd_8Ni_5Co_2$ alloy by selective laser melting. *Addit. Manuf.* **2016**, *6*, 1–5. [CrossRef]
14. Prashanth, K.G.; Scudino, S.; Chaubey, A.K.; Löber, L.; Wang, P.; Attar, H.; Schimansky, F.P.; Pyczak, F.; Eckert, J. Processing of Al-12Si-TNM composites by selective laser melting and evaluation of compressive and wear properties. *J. Mater. Res.* **2016**, *31*, 55–65. [CrossRef]
15. Sun, Z.; Tan, X.; Tor, S.B.; Yeong, W.Y. Selective laser melting of stainless steel 316L with low porosity and high build rates. *Mater. Des.* **2016**, *104*, 197–204. [CrossRef]
16. Pauly, S.; Löber, L.; Petters, R.; Stoica, M.; Scudino, S.; Kühn, U.; Eckert, J. Processing metallic glasses by selective laser melting. *Mater. Today* **2013**, *16*, 37–41. [CrossRef]

17. Suryawanshi, J.; Prashanth, K.G.; Scudino, S.; Eckert, J.; Prakash, O.; Ramamurty, U. Simultaneous enhancements of strength and toughness in an Al-12Si alloy synthesized using selective laser melting. *Acta Mater.* **2016**, *115*, 285–294. [CrossRef]
18. Prashanth, K.G.; Scudino, S.; Eckert, J. Defining the tensile properties of Al-12Si parts produced by selective laser melting. *Acta Mater.* **2017**, *126*, 25–35. [CrossRef]
19. Prashanth, K.G. Selective Laser Melting of Al-12Si. Ph.D. Thesis, Technische Universität Dresden, Dresden, Germany, 2014.
20. Prashanth, K.G.; Scudino, S.; Klauss, H.J.; Surreddi, K.B.; Löber, L.; Wang, Z.; Chaubey, A.K.; Kühn, U.; Eckert, J. Microstructure and mechanical properties of Al-12Si produced by selective laser melting: Effect of heat treatment. *Mater. Sci. Eng. A* **2014**, *590*, 153–160. [CrossRef]
21. Chatterjee, R.P. Selective Laser Melting of Co-Cr-Mo Alloys. Master of Technology Thesis, Indian Institute of Technology Kharagpur, West Bengal, India, 2015.
22. Attar, H.; Prashanth, K.G.; Chaubey, A.K.; Calin, M.; Zhang, L.C.; Scudino, S. Comparison of wear properties of commercially pure titanium prepared by selective laser melting and casting processes. *Mater. Lett.* **2015**, *142*, 38–41. [CrossRef]
23. Löber, L. Selektives Laserstrahlschmelzen von Titanaluminiden und Stahl. PhD Thesis, Technische Universität Dresden, Dresden, Germany, 2015.
24. Prashanth, K.G.; Löber, L.; Klauss, H.; Kühn, U.; Eckert, J. Characterization of 316L steel cellular dodecahedron structures produced by selective laser melting. *Technologies* **2016**, *4*, 34. [CrossRef]
25. Scudino, S.; Unterdörfer, C.; Prashanth, K.G.; Attar, H.; Ellendt, N.; Uhlenwinkel, V.; Eckert, J. Additive manufacturing of Cu-10Sn bronze. *Mater. Lett.* **2015**, *156*, 202–204. [CrossRef]
26. Prashanth, K.G.; Debalina, B.; Wang, Z.; Gostin, P.F.; Gebert, A.; Calin, M.; Kühn, U.; Kamaraj, M.; Scudino, S.; Eckert, J. Tribological and corrosion properties of Al-12Si produced by selective laser melting. *J. Mater. Res.* **2014**, *29*, 2044–2054. [CrossRef]
27. Wang, X.J.; Zhang, L.C.; Fang, M.H.; Sercombe, T.B. The effect of atmosphere on the structure and properties of a selective laser melted Al-12Si alloy. *Mater. Sci. Eng. A* **2014**, *597*, 370–375. [CrossRef]
28. Li, X.P.; Wang, X.J.; Saunders, M.; Suvorova, A.; Zhang, L.C.; Liu, Y.J.; Fang, M.H.; Huang, Z.H.; Sercombe, T.B. A selective laser melting and solution heat treatment refined Al-12Si alloy with a controllable ultrafine eutectic microstructure and 25% tensile ductility. *Acta Mater.* **2015**, *95*, 74–82. [CrossRef]
29. Siddique, S.; Imran, M.; Wycisk, E.; Emmelmann, C.; Walther, F. Influence of process-induced microstructure and imperfections on mechanical properties of AlSi12 processed by selective laser melting. *J. Mater. Process. Technol.* **2015**, *221*, 205–213. [CrossRef]
30. Alsalla, H.; Hao, L.; Smith, C. Fracture toughness and tensile strength of 316L stainless steel cellular lattice structures manufactured using the selective laser melting technique. *Mater. Sci. Eng. A* **2016**, *669*, 1–6. [CrossRef]
31. Kajima, Y.; Takaichi, A.; Nakamoto, T.; Kimura, T.; Yogo, Y.; Ashida, M.; Doi, H.; Nomura, N.; Takahashi, H.; Hanawa, T.; et al. Fatigue strength of Co-Cr-Mo alloy clasps prepared by selective laser melting. *J. Mech. Behav. Biomed. Mater.* **2016**, *59*, 446–458. [CrossRef] [PubMed]
32. Tang, M.; Pistorius, P.C. Oxides, porosity and fatigue performance of $AlSi_{10}Mg$ parts produced by selective laser melting. *Int. J. Fatigue* **2017**, *94*, 192–201. [CrossRef]
33. Rosenthal, I.; Stern, A.; Frage, N. Strain rate sensitivity and fracture mechanism of $AlSi_{10}Mg$ parts produced by selective laser melting. *Mater. Sci. Eng. A* **2017**, *682*, 509–517. [CrossRef]